



NUMERICAL ANALYSIS AND OPTIMIZATION OF A WINGLET SWEEP ANGLE AND WINGLET TIP CHORD FOR IMPROVEMENT OF AIRCRAFT FLIGHT PERFORMANCE

Ali J. Dawood AL-KHAFAJI ^{1,2} , Gennady S. PANATOV ¹, Anton S. BOLDYREV ²

¹ Southern Federal University, Rostov-on-Don, Russia

² University of Technology - Iraq

* Corresponding author, e-mail: alhafadzhi@sfedu.ru

Abstract

In this paper, a study of the effect of winglet sweep angle and winglet tip chord of the aircraft wing on the aerodynamics performances and how to improve it are carried out, assuming Cant angle 60°, winglet height = 3.5 m, Toe angle = -5°, and Twist angle = +5°. Different sweep angles tested (-25°, -15°, 0°, +15°, +25°, +35°, and +45°) and winglet tip chord (0.25, 0.375, and 0.5 m). Four Angle of attack is presented (0°, 3°, 6°, and 9°). The aerodynamics properties of the wing were measured in terms of calculated lift to drag ratio to decide which wing has a high value of lift and lower drag. All models of a wing (eighty-four models) are drawn for 3D using the SOLIDWORKS program. Boeing 737-800 wing dimensions were used. All models of a wing were analyzed using ANSYS FLUENT. The results showed that sweep angle and winglet tip chord of the winglet by changing their configuration can improve aerodynamic performance for various attack angles. The maximum value of the lift to drag ratio was obtained with a sweep angle -15°, winglet tip chord 0.375m, and angle of attack 3°.

Keywords: lift, drag, lift and drag coefficient, aircraft wing, winglet, angle of attack, sweep angle, SOLIDWORKS, CFD, ANSYS FLUENT.

1. Introduction

Winglets are tiny aerodynamic surfaces that are added to the tips of wings to increase their efficiency. Raked tip, blended winglet, canted winglet, up/down winglet, spiroid, tip feathers, tip fence, and other wingtip device shapes have been developed (1). The main goal of the winglet is to enhance the plane's aerodynamic efficiency by reducing the induced drag generation on the wingtip (2-11). A trailing vortex, also known as a wing vortex, is created by the flow and trails behind the aircraft. This trailing vortex causes induced drag by causing a downwash near the aerodynamic center of lift. Induced Drag is the inviscid drag caused by the trailing vortices' impact on the body's aerodynamic center (sometimes called inviscid drag-due-to-lift) the induced drag coefficient, $C_{D,i}$, is given by (7, 12-15).

$$C_{D,i} = \frac{c_L^2}{\pi e AR} \quad (1)$$

For a finite wing with a generalized lift distribution, Equation 1 gives the induced drag coefficient, or drag due to lift. For wings with a higher aspect ratio, this equation is more accurate. The lifting line model of the wing becomes less true as the wing aspect ratio lowers, and the precision of lifting line-based relationships declines. Induced

drag in addition to parasite drag and wave drag is the component of total drag (in coefficient form)(13):

$$C_D = C_{D,e} + C_{D,w} + C_{D,i} \quad (2)$$

The powerful side wash that occurs at the wingtip is taken advantage of by winglets. The wind hits the vertical winglet at an angle of attack as a result of the side wash, resulting in a sideways force. As a result, as illustrated in fig. 1, each winglet has its own horseshoe vortex system. The winglet vortex system partially cancels the wing-tip vortex at the winglet/wingtip junction, resulting in the primary "tip" vortex forming at the winglet's tip. The downwash impact of this vortex is minimized since it lies above the plane of the main wing. In reality, the winglet alters the trailing vorticity distribution throughout the whole span, reducing downwash and generated drag. Furthermore, as illustrated in fig. 1B, the winglet's side force might include a forward thrust component. This reduces drag as well (16).

Commercial aircraft vortex drag accounts for a substantial fraction of aircraft cruise drag, so ideas resulting in a decrease in vortex drag will have a huge impact on fuel consumption, the hundreds of millions of dollars expended annually on fuel by airlines, and their environmental impact. At low speeds, vortex drag is much more important, where vortex drag usually accounts for 80-90 % of the

climb drag of the aircraft under critical take-off conditions (17). The use of winglets to enhance aircraft aerodynamic performance has been the aim of several experiments, beginning with the early work of Whitcomb (18). The Whitcomb winglet is a tip device that extracts energy from the wingtip vortex. The mechanism reduces the strength of the tip vortex and converts the energy into forward propulsion (19). Whitcomb produced a general design approach built on numerical equations, physical flow requirements, and simulation of its overall approach to aerodynamics for the basic design of winglets (20). Whitcomb's research on winglets found that a near-vertical winglet reduces drag nearly twice as much as a horizontal span extension for the same increase in bending moment on the inboard wing. This recommendation was based on the findings of wind-tunnel experiments, in which the winglet and horizontal span extension configurations were meant to be designed so that the root bending moment was comparable (21). A typical example is depicted in fig. 2A. Winglets of this and other types have been fitted to many civil aircraft, ranging from business jets to very large airliners. Fig. 2B, C shows the fundamental principle of the winglet. A secondary flow tends to emerge from the high-pressure zone under the wing near the wingtip to the comparatively low-pressure region on the top surface of all subsonic wings (fig. 2B) (10).

In general, winglet height, sweep angle, cant angle, curvature radius, toe angle, and twist angle are the parameters considered for the construction of a winglet (22). The winglet's sweep angle is often supposed to vary the L/D ratio, but the unwanted interference effect that it could produce at the wing-winglet contact must be taken into account. As the cant and span parameters, this parameter is not supposed to have a high effect, but its analysis is still needed since it may be an important configuration to

consider for the efficiency of the aircraft sector (23, 24).

2. LITERATURE SURVEY

Kazim (25) the researchers for the Office National d'Etudes et de Recherches Aéropatiales (ONERA) M6 wing, determine the optimal winglet orientation. Studies the effect of Cant and sweep winglet angles on aerodynamic performance, For varied attack angles, minor changes in the winglet arrangement can increase aerodynamic performance. According to their dimension and assumption best lift to drag ratio at Cant angle of 30° and sweep angle of 65° which rise 5.33% increases in L/D. the toe-out -5° at AOA 3° which was 2.53% better than the zero-toe angle winglet.

Guerrero (26) the researchers analyzing the effect of cant and sweep angle of the winglet on the aerodynamic performance of a wing at Mach numbers of 0.3 and 0.8395 and variable values angle of attack to different flight phases (take-off, climb, descent, and cruise conditions). the results show the large value of winglet sweep angle and different value of cant angle has a positive effect on the aerodynamic performance of a wing at both value of Mach number and at a cant angle equal to 80° we get maximum lift coefficient and reducing in the slope of the lift curve but this value better than the value of the original wing model and Sweep angle improvement is primarily due to a combination of reduced parasite drag, reduced wave drag at high Mach numbers, and the effect of the winglet's inboard lift power.

Saini (27) winglet cant and sweep angle for Cessna 152 designs and analyze to increase the aerodynamic efficiency of the wing. wing model designed in CATIA V5 for different cant and sweep angles versus different angles of attack. The ANSYS

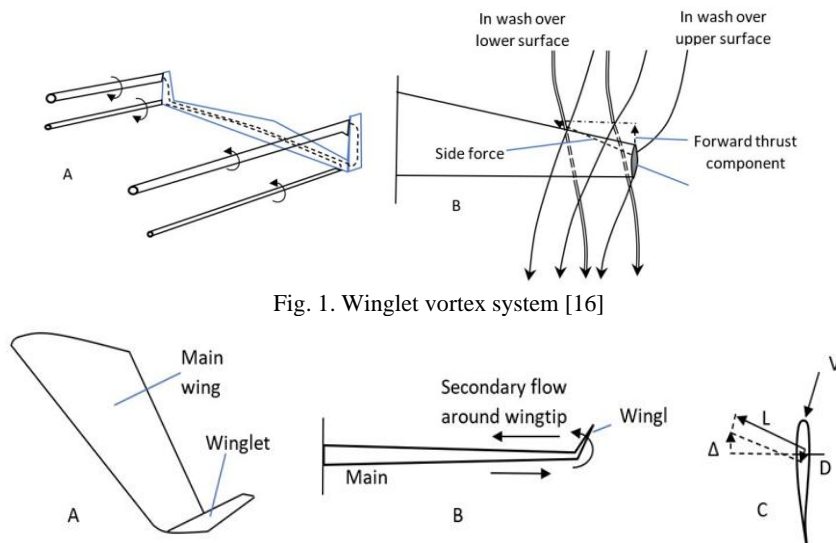


Fig. 1. Winglet vortex system [16]

Fig. 1. Winglet, A) Winglet attached to wingtip, b) secondary flow around wingtip, c) force on winglet (10)

FLUENT was used to analyze the model at sea level conditions using K- ω SST turbulent model.

Guerrero (28) the aim is to improve the aerodynamics parameter by using winglet cant angle (0°, 15°, 45°, and 80°), Winglet sweep angle (30°, 45°, and 60°), angle-of-attack (0°, 2°, 4°, 6°, 8°, and 10°), and Mach number of 0.8395, and The winglet span used corresponds to 20% of the wingspan of the original Onera M6 wing. For all cases studied, the axis is located 40 mm away from the wingtip, the curvature radius is no more than 30 mm, and all models are designed for cruise and cruise climb conditions, it can also be used as a load alleviation tool in the event of heavy gusts or turbulence. The result shows that using variable cant angle for a different angle of attack values (AOA) has a positive effect on drag reduction, also It was discovered that large winglet sweep angle values boost the aerodynamic efficiency of winglet configurations. The study can be more accurate by defining another parameter such as toe-angle, taper ratio, and span.

Amiryants (29) The effect of active winglets on the wing's aeroelastic characteristics was investigated. High sweep angles (back and forward) and is positioned in the same plane as the main wing are the distinguishing characteristics of the winglets in question. The use of such winglets provides for greater control efficiency and lower loads in certain flying regimes and the qualities of flutter were also examined. A raked wingtip that extends beyond the wingspan and is in the same plane as the wing but with a slightly greater (by 5-10%) leading edge (LE) sweep angle than the wing. ARGON interdisciplinary software was used to do the analysis.

3. LIFT AND DRAG CALCULATIONS

The wing is the primary source of aerodynamic force in an airplane, and wing lift acts in the plane of symmetry normal to the direction of flight (30). In the basic design and performance studies of airplanes, lift and drag coefficients play a significant role. Consider a plane flying at a constant, level (horizontal) altitude. The weight W operates vertically downward in this situation. The lift L works perpendicular to the relative wind V_∞ and acts vertically upward (by definition). In order to keep the plane level in flight,

$$L = W \quad (3)$$

The drag D and the thrust T from the propeller are both parallel to V . When flying at a constant speed (without accelerating),

$$T = D \quad (4)$$

Note that the magnitudes of L and W are substantially bigger than the magnitudes of T and D in most normal flying conditions. The lift force is generated when a solid object and a fluid move in

opposite directions. The lift force operates perpendicular to the direction of the fluid's flow, whereas the drag force acts parallel to it.

$$\text{Let } q_\infty = \frac{1}{2} \rho V_\infty^2 \quad (5)$$

Lift coefficient:

$$C_L = \frac{L}{q_\infty S} \quad (6)$$

Drag coefficient:

$$C_D = \frac{D}{q_\infty S} \quad (7)$$

The vertical lift force is created by air flowing past the wing. The pressure differential between the top and lower surfaces of the airfoil is related to lift. The lift force occurs because the pressure on the wing's lower surface is larger than the pressure on the upper surface, since the force applied by a fluid on an object may be defined as the product of pressure and area. The lift force generated by an aircraft's wing is proportional to its form and tilt in relation to the air stream. The angle of attack (AOA) of an airfoil is its inclination, and the lift force will normally expand with AOA up to a point known as the stall condition [7, 10, 11, 31, 32].

In a wide range of industrial applications, such as turbomachinery, wind turbine aerodynamics, helicopter blade rotors, and maneuverable wings, predictions of complicated flow fields incorporating both static and dynamic stall are necessary. The process of surpassing the standard static stall angle is known as dynamic stall [33]. The C_L generated by the airfoil typically rises linearly as AOA increases up to a particular degree. This moment is referred to as the "critical AOA." The wing provides maximum lift (for a given velocity, density, and wing area) at the critical AOA, but the airflow over the wing begins to split from the top surface at the same moment. Lift drops when the AOA is raised beyond the critical AOA, and the wing is termed stopped. The airflow will eventually separate from the wing's top surface, resulting in a total loss of lift [14, 34, 35]. Figure 3, show the relationship between the coefficients of lift and drag at various angles of attack, both coefficients increase with increasing angles of attack to a specific point lift coefficient stall then decreases, while the drag coefficient continues to increase with AOA.

4. LIFT TO DRAG RATIO CALCULATIONS

The aerodynamicist's purpose is to minimize drag to the minimum where the lift-to-drag ratio improves as the drag is reduced. For an efficient design, aircraft designers aim for the optimum possible lift-to-drag ratio (i.e., a metric of lowest fuel use). The lift-to-drag ratio one of the most essential aspects of a vehicle's aerodynamic performance is the lift-to-drag ratio, which is a measure of a

vehicle's aerodynamic efficiency, its ability to produce lift in relation to the drag.

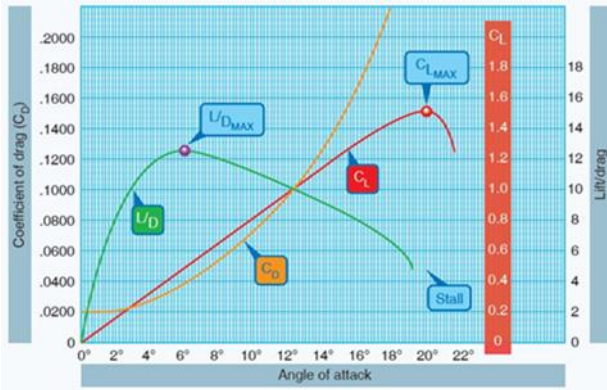


Fig. 3. Coefficients of lift and drag at various angles of attack [36]

$$E = \frac{L}{D} = \frac{C_L}{C_D} \quad (8)$$

It has a direct effect on the range and cross-range capabilities of a re-entry spacecraft that must reach its nominal landing spot by unpowered flight at the end of a space mission. which is controlled by the Mach number, Reynolds number, and attack angle (or the lift coefficient). If both the Mach and Reynolds numbers are known, the aerodynamic efficiency with regard to the lift coefficient reaches its maximum at the point where the straight line from the origin is tangent to the polar diagram. The size and shape of an aircraft's wing have a significant impact on lift and drag. Airspeed affects lift and drag, as well as the lift-to-drag ratio. (13, 14, 19, 37, 38).

5. DESCRIPTION OF MODELS

Eighty-four models are built by using SOLIDWORKS software program and analyzed with ANSYS (Fluent) software program. In this project, different sweep angle (positive and negative) is used (-25, 0, 15, 25, 35, and 45°) and winglet tip chord (0.25, 0.375, and 0.5 m) to build models in show example of this models with different sweep angle and winglet tip chord from the eighty-four models. Fixed Cant angle 60°, winglet span 3.5 m were assumed and a sample winglet with Toe angle = -5°, and Twist angle = +5° shape as in Fig. 3 "a and b" respectively, Fig. 4 show wing shape with a different view orientation drawing in SOLIDWORKS software program with wing dimensions, root Chord (theoretical, at Body Centerline) - 18 feet and 9 inches (5.71 M), mean Aerodynamic Chord (basic wing only) 13 feet and 0 inch (3.96 M), tip Chord (theoretical) - 4 feet and 1.25 inches (1.25 M), planform Taper Ratio, Tip Chord (Root Chord) - 0.219, sweepback (at the 25 percent chord line) - 25.03 degrees. All model builds with four Angle of attack AOA (0°, 3°, 6°, and 9°). Assume that the model: - Space 3D Time Steady

Viscous SST k-omega. Velocity Magnitude (m/s) 230 wing Condition. Reference value: - Boeing 737-800, typical cruising altitude 35,000 ft. with cruising speed 0.78 Mach number, temperature -51 (°C), density: 1.5915 (kg/m³), dynamic viscosity: 1.4584E-5 (kg/m.s), pressure: 3.46 (pascal).

6. ANALYSIS RESULTS

CFD simulations (ANSYS FLUENT) have been done for the eighty-four wing models and then comparing the aerodynamics characteristics of lift coefficient CL, lift force, drag coefficient CD, drag force. The values of CL, CD depend on the shape, inclination, and flow conditions. In the shape, two kinds of parameters are used, first, fixed-parameters like a wing with multi airfoil section (for root we used b737a-il, mid-span b737b-il, b737 c-il, and tip b737d-il), with all dimensions that used in Boeing 737, Cant angle 60°, winglet height = 3.5 m, Toe angle = -5°, and Twist angle = +5°. Second, variable parameters like sweep angles (-25°, -15°, 0°, +15°, +25°, +35°, and +45°) and winglet tip chord (0.25, 0.375, and 0.5 m). In inclination, four Angle of attack AOA (0°, 3°, 6°, and 9°) were used. flow conditions are the same for all models.

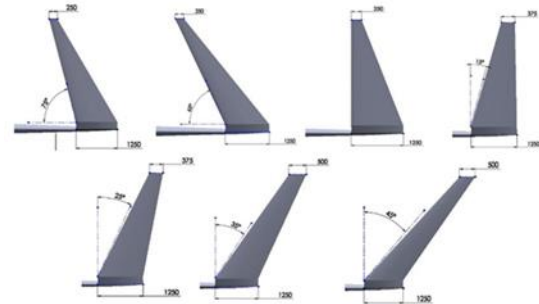


Fig. 2. Wing shape with a different winglet sweep angle & winglet tip chord

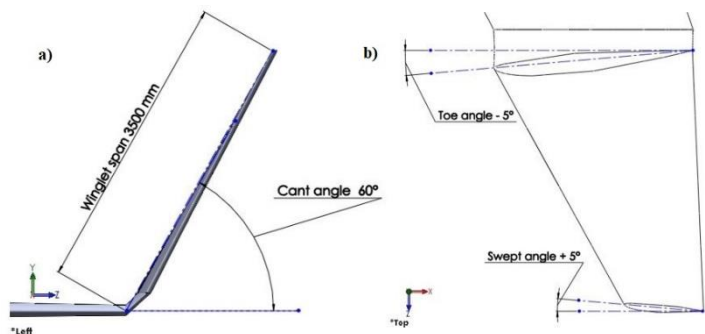


Fig. 3. Winglet assumption and shape

The value of lift and drag force was calculated for all wing models (eighty-four models). The lift and drag force values are increasing with increasing the angle of attack and these results are logical and match with references shown in section 3 "The CL

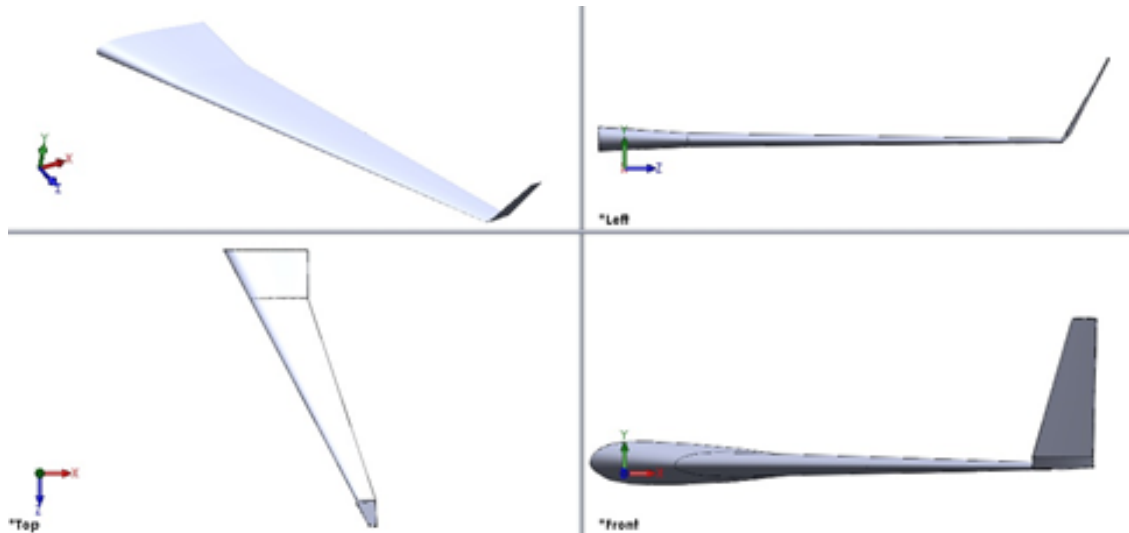


Fig. 4. Wing shape with a different view orientation

and C_D generated by the airfoil typically rises linearly as AOA increases up to a particular degree". Four values of angle of attack (0° , 3° , 6° , and 9°) were used, and the two values does not reach the stall point. In lift force the values of models are almost similar, the difference can see more clearly in drag force, Figure 7.

In Table (1, 2), three chords' measurements (0.25, 0.375, and 0.5 m) are used in models, the maximum and minimum values of lift and drag are occurred in winglets with tip chords equal to 0.5 m knowing that wingtip chord equal to 1.25 m. The maximum lift occurs at a sweep angle equal to -15° and maximum drag at a sweep angle equal to -25° , the two angles are forward-sweep winglet angles.

The calculation of lift and drag force gives us an indication for the behavior of aerodynamics performance of all wing models but is not obvious, some models have a high value of lift but at the same time has a high value of drag and vice versa, so lift to drag ratio (L/D) is calculated to decide which model has better aerodynamics performance.

Figure 8, showed the lift to drag ratio for all models and the maximum lift to drag ratio between 3° to 5° , it is worth mentioning the flight phase is the cruise phase because usually consumes the majority of a flight, and it is rationality. The difference between the maximum and minimum values is huge. Table (3) showed also the maximum lift to drag ratio occurs at a sweep angle equal to -15° and the minimum lift to drag ratio at a sweep angle equal to -25° , the two angles are forward-sweep winglets angles. The maximum value of lift to drag ratio occur in winglet with tip chords equal to 0.375 m and minimum at chord equal to 0.5 m.

Figure 9, shows two models selected from CFD simulation which represent the maximum and minimum lift to drag ratio values, showing the vortex generation and streamline at the end of every

winglet which can be created the induced drag and reduce the aerodynamics efficiency of the wing.

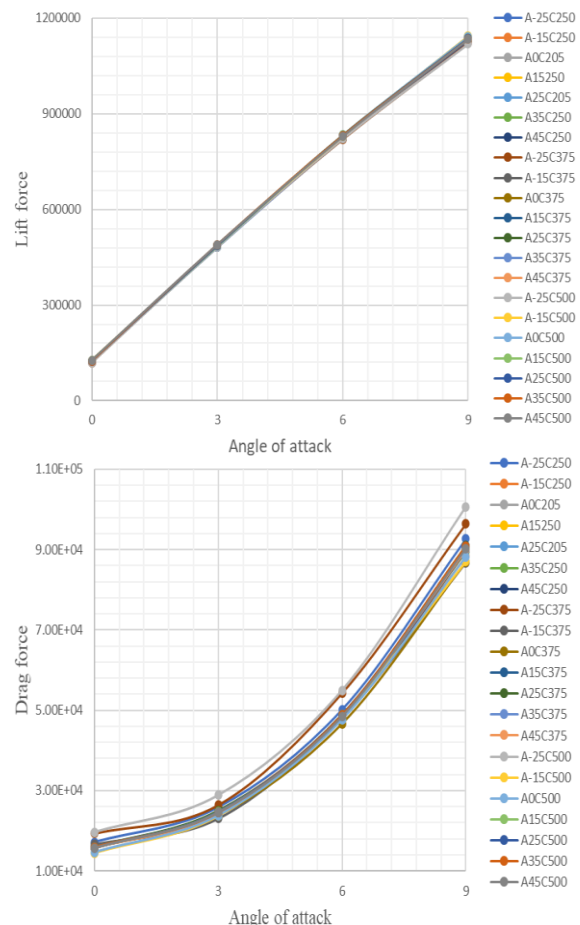


Fig. 5. Lift and drag force of a wing with different winglet sweep angle and winglet tip

Table (1) Lift force value

Function	Value	Description
Max. lift	1144498.80	Sweep angle -15°, Winglet tip chord 0.5m Angle of attack 9°
Min. lift	118869.29	Sweep angle -25°, Winglet tip chord 0.5m Angle of attack 0°

Table (2) Drag force value

Function	Value	Description
Max. drag	100634.84	Sweep angle -25°, Winglet tip chord 0.5m Angle of attack 9°
Min. drag	14436.53	Sweep angle -15°, Winglet tip chord 0.5m Angle of attack 0°

Table (3) Lift to drag ratio value

Function	Value	Description
Max. L/D	20.98	Sweep angle -15°, Winglet tip chord 0.375m Angle of attack 3°
Min. L/D	6.04	Sweep angle -25°, Winglet tip chord 0.5m Angle of attack 0°

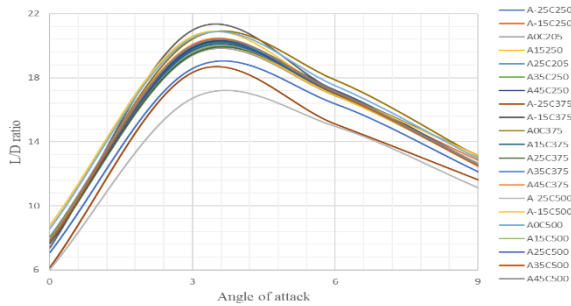


Figure 9A represents the maximum lift to drag ratio value with minimum tip vortex compared with Figure 9B which shows maximum vortex, and also the streamline between the two models that show the airflow around the winglets. So, for our model dimension, the reference value, and our select winglet type we get these values, which can differ when we change any element.

Fig. 6. Lift to drag ratio of a wing with different winglet sweep angle and winglet tip chord versus different angle of attack

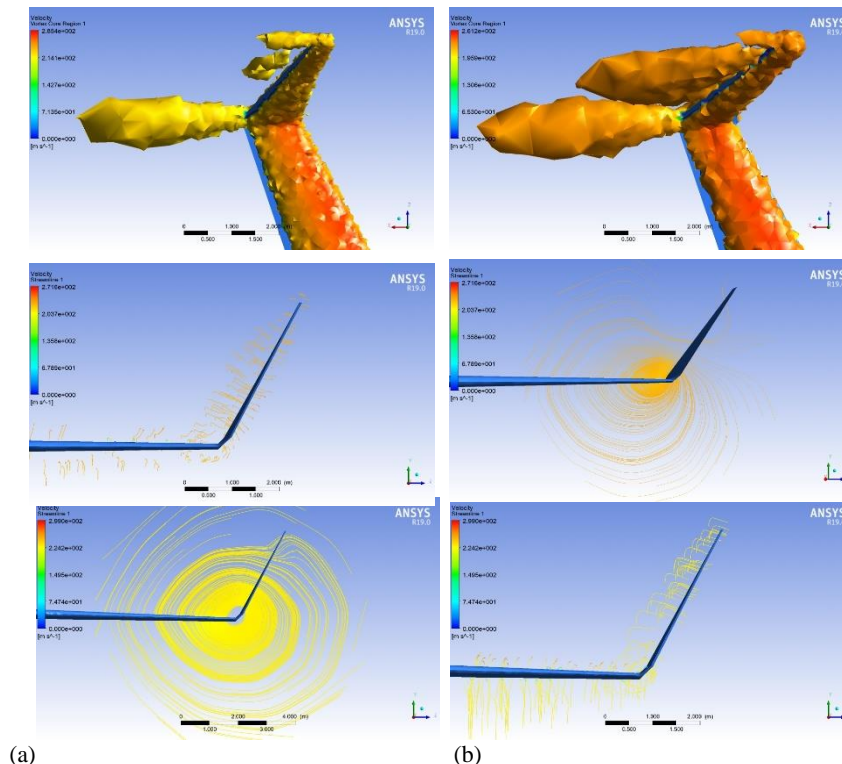


Fig. 7. Wing velocity vortex core and velocity streamline for the a) maximum value b) minimum value of lift to drag ratio

7. CONCLUSION

Simulation is one of the most effective ways to predict the behavior of aerodynamic performance of the wing. Let us modify any suggested design of the wing in a way to increase the lift force with decreases the drag force which reduces the money and time to designer. This paper describes the influence of changing the winglet sweep angle and winglet tip chord versus angle of attack on wing aerodynamic performance. Results show that the maximum L/D ratio (which presents the optimal value of our model), sweep angle -15° , winglet tip chord 0.375m, and angle of attack 3° . The minimum value is sweep angle -25° , winglet tip chord 0.5m, and angle of attack 0° , the difference in percentage equal to 111% difference with these results can minimize fuel consumption leading to saving money and reducing harmful gases.

Unlike the mainstream in the civilian airplane, results show a forward winglet sweep angle due to the CFD simulation by using ANSYS FLUENT, is not the final option of designer, they must check this result with another simulation of the model with structural and material demand to decide the final choices of the wing parameter.

Author contributions: *research concept and design, A.J.D.A-K., G.S.P., A.S.B.; Collection and/or assembly of data, A.J.D.A-K.; Data analysis and interpretation, A.J.D.A-K., G.S.P., A.S.B.; Writing the article, A.J.D.A-K.; Critical revision of the article, A.J.D.A-K., G.S.P. A.S.B.; Final approval of the article, A.J.D.A-K., G.S.P., A.S.P.*

Declaration of competing interest: *The authors declare that they have no known competing financial interests or personal relationships that could have appeared to influence the work reported in this paper.*

REFERENCES

- Chattot JJ, Hafez M. Theoretical and applied aerodynamics: Springer. 2015.
- Bourdin P, Gatto A, Friswell M. Aircraft control via variable cant-angle winglets. *Journal of Aircraft*. 2008;45(2):414-23. <https://doi.org/10.2514/1.27720>.
- Beechook A, Wang J, editors. Aerodynamic analysis of variable cant angle winglets for improved aircraft performance. 2013 19th International Conference on Automation and Computing; 2013.
- Faye R, Laprete R, Winter M. Blended winglets. *Aero*, Boeing. 2002:17.
- Croucher P. JAR professional pilot studies: Lulu. com; 2004.
- Sanders B, Eastep F, Forster E. Aerodynamic and aeroelastic characteristics of wings with conformal control surfaces for morphing aircraft. *Journal of aircraft*. 2003;40(1):94-9. <https://doi.org/10.2514/2.3062>.
- Anderson Jr JD. Fundamentals of aerodynamics: Tata McGraw-Hill Education; 2010.
- Larson G. How Things Work: Winglets. *Air & Space Magazine*. 2001:09-1.
- Raymer D. Aircraft Design: A Conceptual Approach, Education Series, American Institute of Aeronautics and Astronautics. Inc, Reston, VA. 2006.
- Houghton EL, Carpenter PW. Aerodynamics for engineering students: Elsevier; 2003.
- Kundu AK, Price MA, Riordan D. Conceptual Aircraft Design: An Industrial Approach: John Wiley & Sons; 2019.
- Carichner GE, Nicolai LM. Fundamentals of Aircraft and Airship Design, Volume 2–Airship Design and Case Studies: American Institute of Aeronautics and Astronautics, Inc.; 2013.
- Corda S. Introduction to aerospace engineering with a flight test perspective: John Wiley & Sons; 2017.
- Miele A. Flight mechanics: theory of flight paths: Courier Dover Publications; 2016.
- Moran J. An introduction to theoretical and computational aerodynamics: Courier Corporation; 2003.
- Barnard RH, Philpott DR. Aircraft flight: a description of the physical principles of aircraft flight: Pearson education; 2010.
- Kroo I. Nonplanar wing concepts for increased aircraft efficiency. VKI lecture series on innovative configurations and advanced concepts for future civil aircraft. 2005.
- Elham A, van Tooren MJ. Winglet multi-objective shape optimization. *Aerospace Science and Technology*. 2014;37:93-109.
- Marqués P, Da Ronch A. Advanced UAV Aerodynamics, Flight Stability and Control: Novel Concepts, Theory and Applications: John Wiley & Sons; 2017.
- Hallion R. NASA's Contributions to Aeronautics: National Aeronautics and Space Administration; 2010.
- McLean D. Understanding aerodynamics: arguing from the real physics: John Wiley & Sons; 2012.
- Papadopoulos C, Schmid M, Kaparos P, Misirlis D, Vlahostergios Z. Numerical Analysis and Optimization of a Winglet for a Small Horizontal Wind Turbine Blade. *Chemical Engineering Transactions*. 2020;81:1321-6. <https://doi.org/10.3303/CET2081221>.
- Vandam CP, Roskam J. Analysis of nonplanar wing-tip-mounted lifting surfaces on low-speed airplanes. 1983.
- Cancino Queirolo MA. Impact of Morphing Winglets on Aircraft Performance. 2018.
- Kazim AH, Malik AH, Ali H, Raza MU, Khan AA, Aized T, et al. CFD analysis of variable geometric angle winglets. *Aircraft Engineering and Aerospace Technology*. 2021;94(2):289-301. <https://doi.org/10.1108/AEAT-10-2020-0241>.
- Guerrero JE, Sanguineti M, Wittkowski K. Variable cant angle winglets for improvement of aircraft flight

- performance. *Meccanica*. 2020;55(10):1917-1947.
<https://doi.org/10.1007/s11012-020-01230-1>.
27. Saini V, Bhargav NS, Mohiddinsha Y, Senthilkumar S. Winglet Design and Analysis for Cessna 152-A Numerical Study. SAE Technical Paper; 2019. Report No.: 0148-7191.
 28. Guerrero J, Sanguineti M, Wittkowski K. CFD study of the impact of variable cant angle winglets on total drag reduction. *Aerospace*. 2018;5(4):126.
<https://doi.org/10.3390/aerospace5040126>.
 29. Amiryants G, Paryshev S, Grigoriev A, editors. Aeroelastic properties of active winglets. 31st Congress of the International Council of the Aeronautical Sciences, ICAS 2018; 2018.
 30. Cook MV. Flight dynamics principles: a linear systems approach to aircraft stability and control: Butterworth-Heinemann; 2012.
 31. Wickert J, Lewis K. An introduction to mechanical engineering: Cengage learning; 2020.
 32. Bertin JJ, Cummings RM. Aerodynamics for engineers: Cambridge University Press; 2021.
 33. Kajishima T, Mohamad F. Large-eddy simulation of unsteady pitching aerofoil using a oneequation subgrid scale (SGS) model based on dynamic procedure. *Journal of Mechanical Engineering (JMeche)*. 2021;18(1):157-73.
<https://doi.org/10.21491/jmeche.v18i1.15178>.
 34. Boesser CT. The Effects of Angle-of-Attack Indication on Aircraft Control in the Event of an Airspeed Indicator Malfunction. 2013.
 35. Heisler H. Advanced vehicle technology: Elsevier; 2002.
 36. Duncan JS. Pilot's handbook of aeronautical knowledge. US Department of Transportation Federal Aviation Administration Flight Standards Service. 2016:25-32.
 37. Hull DG. Fundamentals of airplane flight mechanics: Springer; 2007.
 38. Kundu AK. Aircraft design: Cambridge University Press; 2010.

Received 2022-01-18

Accepted 2022-05-27

Available online 2022-06-06